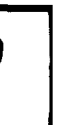

National Défense
Defence nationale

KALMAN FILTER-BASED ARCHITECTURES FOR INTERFERENCE EXCISION (U)

by

Brian Kozminchuk

DEFENCE RESEARCH ESTABLISHMENT OTTAWA
REPORT NO. 1118

Canada

December 1991
Ottawa

National Defence / Défense nationale

KALMAN FILTER-BASED ARCHITECTURES FOR INTERFERENCE EXCISION (U)

by

Brian Kozminchuk
Communications Electronic Warfare Section
Electronic Warfare Division

DEFENCE RESEARCH ESTABLISHMENT OTTAWA
REPORT NO. 1118

PCN
041LK

December 1991
Ottawa

ABSTRACT

This report presents a novel Kalman filtering approach to the suppression of narrowband interference from direct sequence spread spectrum communications systems. The algorithm is based on the digital phase-locked loop Kalman filter. Because the interference is assumed to be much stronger than either the signal or noise, the Kalman filter locks onto a function related to the interference. The net result is an estimate of the phase of the interference and its amplitude. The algorithm is characterized through computer simulation for the case of narrowband Gaussian noise interference. Examples of the phase- and envelope-tracking capabilties of the algorithm are presented, followed by bit error rate curves for interference bandwidths ranging from 0.5% to 5.0% of the chip rate of the spread spectrum signal . The report concludes with three adaptive architectures. The first is suitable for constant envelope interference; the second is a more general structure; and the third incorporates a decision-feedback structure accompanied with a training sequence.

RÉSUMÉ

Ce rapport présente une nouvelle façon d'effectuer un filtrage de Kalman pour exciser de l'interférence à bande étroite d'un système de communication utilisant des spectres étalés par séquence directe. L'algorithme est basé sur un filtre de Kalman à boucle numérique de verrouillage de phase. L'interférence est sensée être beaucoup plus faible que le signal ou le bruit de façon à ce que le filtre de Kalman se verrouille sur une fonction liée à l'interférence . Il en résulte une évaluation de la phase et de l'amplitude de l'interférence. L' algorithme est caractérisé grâce à une simulation par ordinateur pour le cas où l'interférence prend la forme de bruit gaussien à bande étroite. On présente d'abord des exemples de poursuite de phase et d'enveloppe, puis des courbes du taux d'erreur des bits pour des bandes d'interférence ayant une largeur entre 0.5% et 5.0% du débit numérique du signal à spectre étalé. Le rapport se termine par la présentation de trois architectures adaptives. La première convient aux interférences à enveloppe constante, la deuxième est une structure plus générale et la troisième incorpore une structure de rétroaction décisionnelle et une séquence d'essai.

EXECUTIVE SUMMARY

This report presents a Kalman filtering algorithm that is used for filtering narrowband interferers out of direct sequence spread spectrum signals. These signals are used extensively in military communication systems. The technique described herein applies equally to both Electronic Support Measures (ESM) systems and direct sequence spread spectrum communication sytems. In the former application, the ESM system may be attempting to intercept the spread spectrum signal, but the narrowband interference may be hampering this effort. In the latter application, the spread spectrum communication system may require additional assistance to suppress the interference. Since the open literature has been devoted to this latter case, the material presented here focuses on this application.

One of the attributes of direct sequence spread spectrum communication systems is their ability to combat interference or intentional jamming by virtue of the system's processing gain inherent in the spreading and despreading process. The interference can be attenuated by a factor up to this processing gain. In some cases the gain is insufficient to effectively suppress the interferer, leading to a significant degradation in communications manifested by a sudden increase in bit error rate. If the ratio of interference bandwidth to spread spectrum bandwidth is small, the interference can be filtered out to enhance system performance. However, this is at the expense of introducing some distortion onto the signal. This process of filtering is sometimes referred to as interference excision.

The Kalman filtering algorithm is based on the digital phase-locked loop Kalman filter. Because the interference is assumed to be much stronger than either the signal or noise, the Kalman filter locks onto the interference. The net result is an estimate of the phase and amplitude of the interference.

The algorithm is characterized through computer simulation for the case of narrowband Gaussian noise interference. Examples of the phase- and envelope-tracking capabilties of the algorithm are presented, followed by bit error rate curves for interference bandwidths ranging from 0.5% to 5.0% of the chip rate of the spread spectrum signal. The report concludes with three adaptive architectures. The first is suitable for constant envelope interference; the second is a more general structure; and the third incorporates a decision-feedback structure used in conjunction with a training sequence to stabilize the filter.

Military applications of this work cannot be discussed in this unclassified report.

TABLE OF CONTENTS

LIST OF TABLES

LIST OF FIGURES

1.0 INTRODUCTION

Direct sequence spread spectrum communication systems have an inherent processing gain which can reduce the effects of jammers or unintentional interference. When these intruding signals have a power advantage over the spread spectrum system, a severe degradation in communications results. However, communications can be enhanced somewhat by filtering the interference, particularly if its bandwidth is significantly less than the bandwidth of the spread spectrum signal.

A host of digital filtering algorithms based on time-modelling concepts have been developed over the years to address this problem [1, 2, 3]. The received signal, noise and interference are applied, for example, to a filter matched to a chip and the output is sampled at the chip rate. If one assumes that the resulting sampled data can be modelled as an autoregressive (AR) process, then the AR coefficients or their related lattice reflection coefficients can be determined from, say, the maximum entropy algorithm [4], stochastic gradient algorithms [5], and block and recursive least squares algorithms [6, 7]. Estimates of these coefficients by the above algorithms lead directly to transversal or lattice filter structures, both of which act as whitening filters for the assumed AR process. This approach to suppress interference (or excision as it is sometimes referred to) is possible because of the non-coherency of the signal and noise samples, and the more coherent interference samples resulting from the latter's narrowband nature.

This paper presents a different time-modelling approach to interference excision. A function related to the interference is assumed to have been generated by a second order state-space system to which the extended Kalman filter equations are applied. This results in what has been termed the digital phase-locked loop (DPLL) [8, 9]. There are certain benefits to using the DPLL over its analog counterpart [10]. First, it can be made adaptive, responding to changing interference conditions; and, second, being digital, other DPLL's can be switched in as required to handle more than one interferer.

The outline of the paper is as follows. Section 2.0 describes the spread spectrum communication model. Section 3.1 describes the state-space model which produces a function related to the interference. Section 3.2 presents the Kalman algorithm which is used to estimate the phase of the interference. Another model [11] is also presented, which is slightly different from that in [8]. Section 4.0 describes the interference estimator. Section 5.0 presents simulation results for the case of narrowband Gaussian noise corrupting the spread spectrum signal. The results are presented in terms of bit error rate for various parameter values of the excisor. Finally, the results suggest a strategy to render the algorithm adaptive, which is discussed in Section 6.0.

2.0 MODEL OF THE PN SPREAD-SPECTRUM COMMUNICATION SYSTEM

A BPSK PN spread spectrum system is considered here, the basic elements of which are shown in Fig. 1.

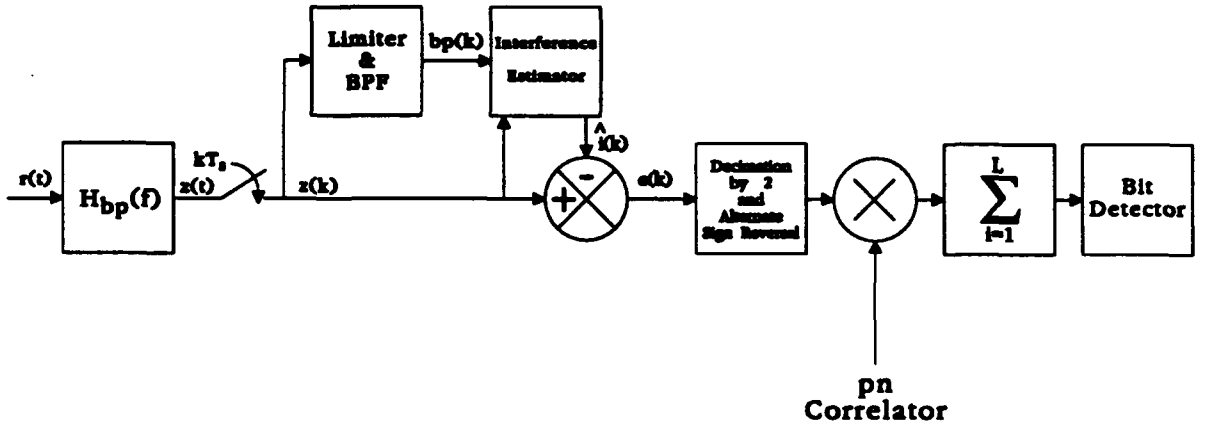

Figure 1: Spread spectrum communications model.

Certain assumptions are made in what follows. These include distortionless transmission, and phase and code synchronization.

The received waveform $r(t)$, consisting of a spread spectrum signal, additive white Gaussian noise, and narrowband interference is applied to a bandpass filter with the transfer function $H_{bp}(f)$, whose output is defined as

$$z(t) = s(t) + n(t) + i(t). \tag{1}$$

The bandpass filter $H_{bp}(f)$, for the application considered in this paper, is assumed to be a filter matched to a chip and centered at the carrier frequency ω_0 of the spread spectrum signal.

The spread spectrum signal, which is of bandwidth B_{ss}, is defined as

$$s(t) = a(t)\cos(\omega_0 t), \tag{2}$$

where

$$a(t) = \sum_{n}\sum_{j=1}^{L} c_{nj} d_n p(t - jT_c - nT_b). \tag{3}$$

The term c_{nj} in Eq. (3) is the code sequence for the n^{th} information bit d_n, T_b is the reciprocal of the bit rate R_b, $p(t)$ is the basic chip pulse of energy E_c, T_c is the reciprocal

of the chip rate R_c, and L is the number of chips per bit, also known as the processing gain.

The noise $n(t)$ is Gaussian and has a power spectral density

$$S_n(f) = \frac{N_0}{2}|H_{bp}(f)|^2, \tag{4}$$

where $N_0/2$ is the power spectral density of the assumed white Gaussian noise from the channel. The interference is generally defined as

$$i(t) = I(t)\cos[\omega_0 t + \theta(t)] \tag{5}$$

and is of bandwidth $B_i << B_{ss}$.

Referring to Fig. 1, the output $z(t)$ of the bandpass filter $H_{bp}(f)$ is bandpass sampled and applied to a bandpass limiter and interference estimator.

Consider the bandpass sampler first. The analog signal $z(t)$ from Eq. (1) is sampled at $f_s = 2R_c$ ($mf_s = \omega_0/2\pi + R_c$ for some integer m), where R_c is the chip rate. The resultant sampled signal is, therefore,

$$z(k) = s(k) + n(k) + i(k), \tag{6}$$

where $s(k)$ consists of the sequence $\{\ldots, 0, (-1)^k E_c, 0, (-1)^{k+2} E_c, \ldots\}$ (recall that coherent bandpass sampling has been assumed), $n(k)$ are uncorrelated Gaussian noise samples of variance $\sigma_n^2 = E_c(N_0/2)$, and $i(k)$ is the sampled version of Eq. (5). The samples $z(k)$ are applied to the interference estimator and interference canceller.

Consider now the branch containing the limiter. Here, $z(k)$ is applied to a bandpass limiter. The input to the limiter is redefined as

$$z(k) = \sqrt{[I(k) + n_1'(k) + a_1'(k)]^2 + [n_2'(k) + a_2'(k)]^2}\cos[\omega_0 k + \theta(k) + \phi_z(k)] \tag{7}$$

where

$$\phi_z(k) = \arctan\left(\frac{n_2'(k) + a_2'(k)}{I(k) + n_1'(k) + a_1'(k)}\right) \tag{8}$$

is a noiselike phase fluctuation on the interferer's phase $\theta(k)$, and is due to the noise and spread spectrum signal. The terms $n_1'(k)$, $n_2'(k)$, $a_1'(k)$, and $a_2'(k)$ are in-phase and quadrature components of the noise and spread spectrum signal with respect to the interference

phase $\theta(k)$. The output of the bandpass limiter is [12]

$$bp(k) = \frac{4A'}{\pi} \cos[\omega_0 k + \theta(k) + \phi_z(k)], \tag{9}$$

where A' is the limiter's output level. This signal is redefined as (letting $A' = \sqrt{2}\pi/4$ for convenience)

$$bp(k) = \sqrt{2} \cos[\omega_0 k + \theta(k) + \phi_z(k)]. \tag{10}$$

It should be noted that for large interference-to-noise ratios in which the interference is of constant envelope, $\phi_z(k)$ in Eq. (9) is approximately Gaussian [12]. The sampled signal in Eq. (10) is what is processed by the Kalman filter, which estimates the phase $\theta(k)$ of the interference.

3.0 KALMAN FILTER ALGORITHM

3.1 STATE SPACE MODEL OF THE INTERFERENCE

The development here follows that in [8]. The analog interference model will be discussed first, followed by its digital counterpart.

A block diagram of the analog state space model which generates the analog version of a function related to $bp(t)$ in Eq. (9) is shown in Fig. 2. The state space equations are defined as

$$\begin{bmatrix} \dot{x}_1(t) \\ \dot{x}_2(t) \end{bmatrix} = \begin{bmatrix} 0 & d \\ 0 & -\alpha \end{bmatrix} \begin{bmatrix} x_1(t) \\ x_2(t) \end{bmatrix} + \begin{bmatrix} 0 \\ \sqrt{K_w} \end{bmatrix} w(t), \tag{11}$$

where $x_1(t)$ and $x_2(t)$ are the phase function and modulating signal state variables of the interference, respectively. In compact form Eq. (11) becomes

$$\dot{\boldsymbol{x}}(t) = \boldsymbol{A}\boldsymbol{x}(t) + \boldsymbol{g}w(t). \tag{12}$$

The interferer's modulating signal $x_2(t)$ is assumed to be generated by applying Gaussian white noise, $w(t)$, of unit variance to an amplifier with gain $\sqrt{K_w}$ followed by a first order low pass filter of bandwidth $\alpha = 2\pi\alpha_f$. The steady state variance of the coloured noise at the output of the lowpass filter is unity if $K_w = 2\alpha$. The output is multiplied by the frequency deviation constant, d, and then integrated to yield the phase function

$$x_1(t) = d \int_0^t x_2(\tau)\, d\tau. \tag{13}$$

An FM type of signal (interferer) is generated by phase modulating a carrier, ω_0, which has been set equal to the carrier of the spread spectrum signal, since any offsets from ω_0 can be incorporated into $x_1(t)$, yielding

$$y(t) = \sqrt{2}\cos[\omega_0 t + x_1(t)]. \tag{14}$$

This signal is corrupted by white Gaussian noise $v(t)$ with power spectral density $N/2$ generally different from $N_0/2$ defined earlier for the communications model in Fig. 1. The result is an FM signal related to the interference in Eq. (9) except for the fact that the noise term is additive here, i.e.,

$$bp(t)' = y(t) + v(t). \tag{15}$$

For large interference-to-signal-plus-noise conditions, the final effect of the additive noise in estimating the phase $x_1(t)$ in Eq. (14) will be similar to the effect of $\phi_z(k)$ in Eq. (9).

Given the observation process $bp'(t)$ from Eq. (15), the objective is to estimate the state $x_1(t)$ and the related state $x_2(t)$, as well as $y(t)$ in Eq. (14). One approximate technique reserved for nonlinear estimation problems [13] is the extended Kalman filter algorithm.

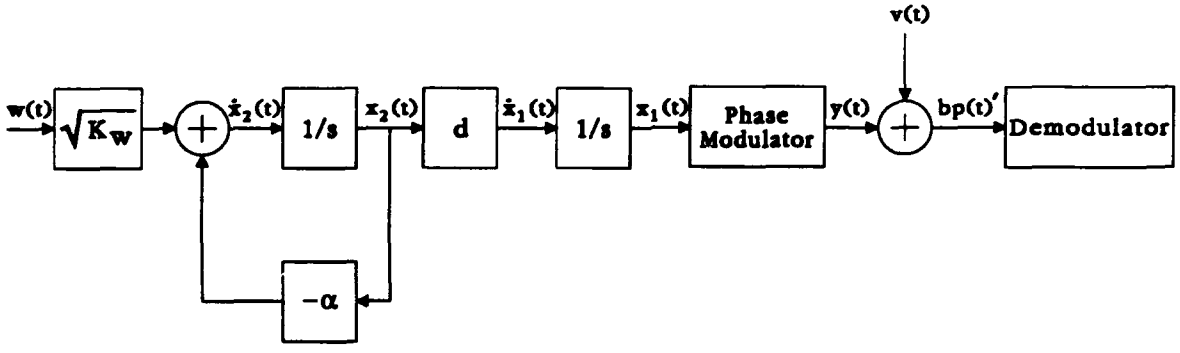

Figure 2: Block diagram of the state space model.

Before the algorithm is presented, the discrete forms of Eqs. (11) and (12) will be stated, namely,

$$\boldsymbol{x}(k+1) = \boldsymbol{\phi}\boldsymbol{x}(k) + \boldsymbol{w}(k), \tag{16}$$

where k represents discrete time,

$$\boldsymbol{\phi} = \begin{bmatrix} 1 & \beta(1-e^{-\alpha T_s}) \\ 0 & e^{-\alpha T_s} \end{bmatrix} = \begin{bmatrix} 1 & \phi_{12} \\ 0 & \phi_{22} \end{bmatrix} \tag{17}$$

and

$$\boldsymbol{w}(k) = \int_{kT_s}^{(k+1)T_s} \boldsymbol{\phi g} w(u)\, du. \tag{18}$$

In Eq. (17), $\beta = d/\alpha$ and is termed the bandwidth expansion ratio in units of $volts^{-1}$ [14]. In Eq. (18), $\boldsymbol{w}(k)$ is a stationary zero-mean white Gaussian vector sequence whose covariance, (i.e., $E\{\boldsymbol{w}(k)\boldsymbol{w}(k)^t\}$), is given by

$$\boldsymbol{V}_w = \int_{kT_s}^{(k+1)T_s} \boldsymbol{\phi g g}^t \boldsymbol{\phi}\, du. \tag{19}$$

Finally, Eq. (14) becomes,

$$bp'(k) = y(k) + v(k), \tag{20}$$

where $y(k)$ is the sampled version of Eq. (14). It has been assumed that $bp'(t)$ from Eq. (15) has been applied to a bandpass filter of bandwidth B, whose output has been sampled at a rate so as to yield uncorrelated noise samples $v(k)$ of variance $\sigma_v^2 = B(N/2)$ [9].

The noise covariance matrix, $\boldsymbol{V}_w$, is obtained by substituting Eq. (17) and $\boldsymbol{g}$ from Eq. (12) into Eq. (19) and integrating each term, yielding

$$\boldsymbol{V}_w = \frac{K_w}{2\alpha} \begin{bmatrix} \beta^2\left(4\pi/\gamma - 3 + 4e^{-2\pi/\gamma} - e^{-4\pi/\gamma}\right) & \beta\left(1 - e^{-2\pi/\gamma}\right) \\ \beta\left(1 - e^{-2\pi/\gamma}\right) & 1 - e^{-4\pi/\gamma} \end{bmatrix} \tag{21}$$

where $\gamma = 2\pi/(\alpha T_s)$, which is the ratio of the sampling rate $f_s = 1/T_s$ to the interferer's modulating signal bandwidth α_f. The discrete form of the interference model is shown in Fig. 3.

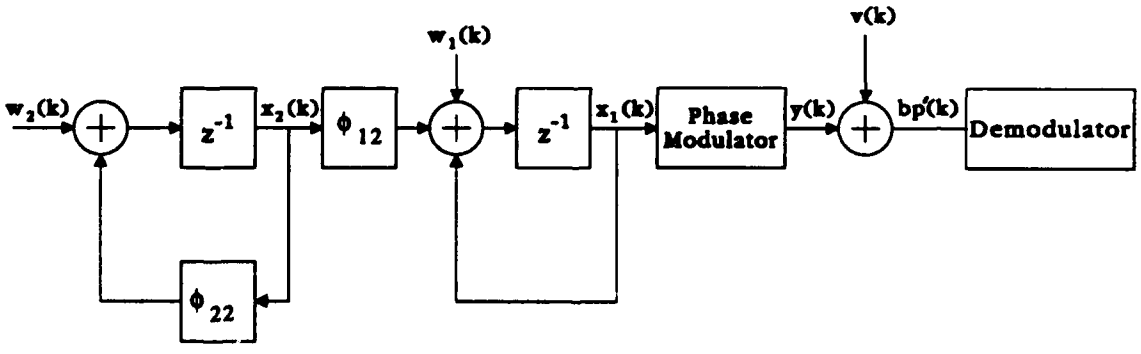

Figure 3: Discrete form of the interference model.

3.2 EXTENDED KALMAN FILTER EQUATIONS

The extended Kalman filter equations [13] can now be applied to the discrete model. The resulting algorithm is as follows:

Initial Conditions:

$$\hat{\boldsymbol{x}}(-1) = E\{\hat{\boldsymbol{x}}(-1)\} = \begin{bmatrix} \mu_1 \\ \mu_2 \end{bmatrix} \tag{22}$$

$$\boldsymbol{V}_{\tilde{\boldsymbol{x}}}(-1) = E\{\tilde{\boldsymbol{x}}(-1)\tilde{\boldsymbol{x}}^t(-1)\} \tag{23}$$

Do for $k = 0$ to T:

$$\hat{\theta}(k|k-1) = \begin{bmatrix} 1 & 0 \end{bmatrix} \boldsymbol{\phi}\hat{\boldsymbol{x}}(k-1) \tag{24}$$

$$\boldsymbol{V}_{\tilde{\boldsymbol{x}}}(k|k-1) = \boldsymbol{\phi}\boldsymbol{V}_{\tilde{\boldsymbol{x}}}(k-1)\boldsymbol{\phi}^t + \boldsymbol{V}_w \tag{25}$$

$$e^{-1}(k|k-1) = \frac{1 - \cos[2\omega_0 k + 2\hat{\theta}(k|k-1)]}{\sigma_v^2 + \begin{bmatrix} 1 & 0 \end{bmatrix} \boldsymbol{V}_{\tilde{\boldsymbol{x}}}(k|k-1) \begin{bmatrix} 1 & 0 \\ 0 & 0 \end{bmatrix} \boldsymbol{V}_{\tilde{\boldsymbol{x}}}(k|k-1) e^{-1}(k|k-1)} \tag{26}$$

$$\boldsymbol{K}(k) = -\boldsymbol{V}_{\tilde{\boldsymbol{x}}}(k) \begin{bmatrix} 1/\sigma_v^2 \\ 0 \end{bmatrix} \sqrt{2}\sin[\omega_0 k + \hat{\theta}(k|k-1)] \tag{27}$$

$$\hat{\boldsymbol{x}}(k) = \boldsymbol{\phi}\hat{\boldsymbol{x}}(k-1) + \boldsymbol{K}(k)[bp'(k) - \sqrt{2}\cos[\omega_0 k + \hat{\theta}(k|k-1)]. \tag{28}$$

In the algorithm $\hat{\boldsymbol{x}}(k)$ is defined as the estimate of the true state vector $\boldsymbol{x}(k)$, $\tilde{\boldsymbol{x}}(k)$ is defined as the post error $\boldsymbol{x}(k) - \hat{\boldsymbol{x}}(k)$, $\boldsymbol{K}(k)$ is the Kalman gain vector, $\boldsymbol{V}_{\tilde{\boldsymbol{x}}}(k) = E\{\tilde{\boldsymbol{x}}(k)\tilde{\boldsymbol{x}}^t(k)\}$ is the post error covariance and $\boldsymbol{V}_{\tilde{\boldsymbol{x}}}(k|k-1) = E\{\tilde{\boldsymbol{x}}(k|k-1)\tilde{\boldsymbol{x}}^t(k|k-1)\}$. Furthermore, Eq. (26) is known as the "coupled equation", since the estimate of the interferer's phase is contained in it. However, this equation can be further approximated as noted in [8]. The approximation is

$$e^{-1}(k|k-1) = \frac{1}{V_{\tilde{\boldsymbol{x}}_{11}}} \left\{ 1 - \sqrt{\frac{\sigma_v^2}{\sigma_v^2 + V_{\tilde{\boldsymbol{x}}_{11}}}} \right\}. \tag{29}$$

It has been shown in [8] that the Kalman algorithm results in a digital PLL. The state space diagram of the DPLL is illustrated in Fig. 4. Observe that the phase estimate

$\hat{\theta}(k|k-1)$ is applied to a phase modulator of frequency ω_0, resulting in a "VCO" signal defined as

$$VCO(k) = -\sqrt{2}\sin(\omega_0 k + \hat{\theta}(k|k-1)). \tag{30}$$

Shifting this signal by $-\pi/2$ radians results in a filtered estimate of $y(k)$ in Eq. (20). Finally, by rearranging the system in Fig. 4 into a transfer function model at steady state, one obtains the system illustrated in Fig. 5 where

$$C = \frac{2\phi_{12}V_{\tilde{x}_{12}}(\infty) + V_{\tilde{x}_{12}}(\infty)}{\sigma_v^2}, \tag{31}$$

$$b = \frac{\phi_{12}V_{\tilde{x}_{12}}(\infty) + V_{\tilde{x}_{12}}(\infty)\phi_{22}}{2\phi_{12}V_{\tilde{x}_{12}}(\infty) + V_{\tilde{x}_{12}}(\infty)}, \tag{32}$$

and

$$a = \phi_{22}. \tag{33}$$

The DPLL consists of a gain C, followed by the loop filter, and integrator. These equations indicate that the gain and loop filter parameters (pole and zero) are linked to the steady state phase variance $V_{\tilde{x}_{11}}(\infty)$, the phase/modulating signal covariance $V_{\tilde{x}_{12}}(\infty)$, the state transition parameters ϕ_{12} and ϕ_{22}, and the variance of the observation noise σ_v^2. Steady state performance ultimately depends on the choices of d, σ_v^2 and T_s of the model.

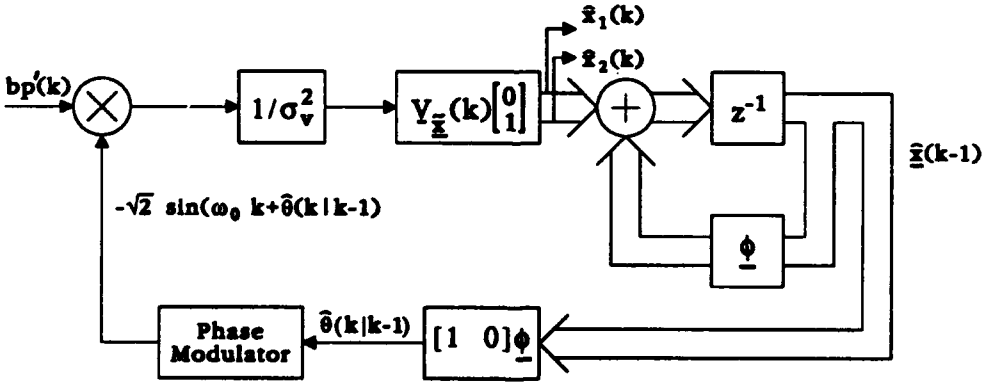

Figure 4: State space representation of the DPLL.

The loop filter shown in Fig. 5 will lead to a steady state error if the phase $x_1(k)$ is a ramp. This loop filter can be changed to one consisting of proportional plus integral control by modifying the interference model [11]. The modification involves replacing the low pass filter by an integrator (i.e., by setting $\alpha = 0$ in A in Eq. (12)). With this change,

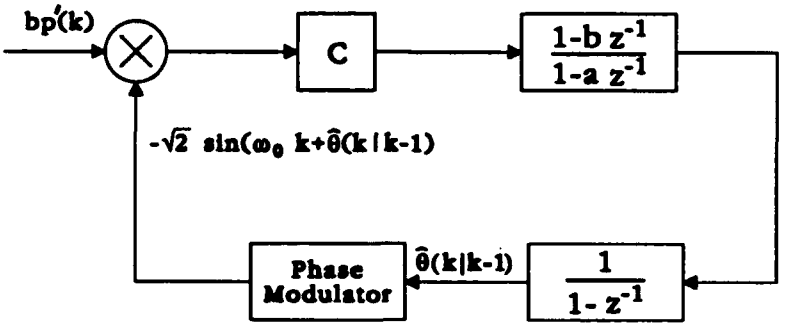

Figure 5: Transfer function model representation of the DPLL.

the state transition matrix ϕ and covariance matrix V_w become, respectively,

$$\phi = \begin{bmatrix} 1 & dT_s \\ 0 & 1 \end{bmatrix} = \begin{bmatrix} 1 & \phi_{12} \\ 0 & \phi_{22} \end{bmatrix} \tag{34}$$

and

$$V_w = K_w \begin{bmatrix} d^2T_s^3 & dT_s^2 \\ dT_s^2 & T_s \end{bmatrix}. \tag{35}$$

Using these terms in the Kalman equations results in a slightly modified algorithm. This is the algorithm that has been used in the simulations in Section 5.0. The transfer function parameters in Eqs. (31) and (32) remain unchanged, but $a = 1$ in Eq. (33).

4.0 THE INTERFERENCE ESTIMATOR

The Kalman algorithm produces a filtered estimate of $y(k)$ in Eq. (20), which can be used as a basis for estimating a sampled version of the the amplitude of $i(t)$ (i.e., $I(k)$ in Eq. (5)). The interference estimator is illustrated in Fig. 6. The output of the multiplier is a baseband term, and is (using Eq. (6)),

$$\begin{aligned} \hat{I}'(k) &= \frac{1}{\sqrt{2}}\Big\{I(k)\cos[\theta(k) - \hat{\theta}(k|k-1)] \\ &+ n(k)\cos[\omega_0 k + \hat{\theta}(k|k-1)] + a(k)\cos[\hat{\theta}(k|k-1)] \\ &+ a(k)\cos[2\omega_0 k + \hat{\theta}(k|k-1)]\Big\}. \end{aligned} \tag{36}$$

Equation (36) consists of four terms: the first term is related to the desired amplitude of the interference; the second is approximately Gaussian baseband noise [14]; and the third and fourth terms are noise-like terms emanating from the spread spectrum signal. The fourth term has been ignored in the simulations, since it has been assumed

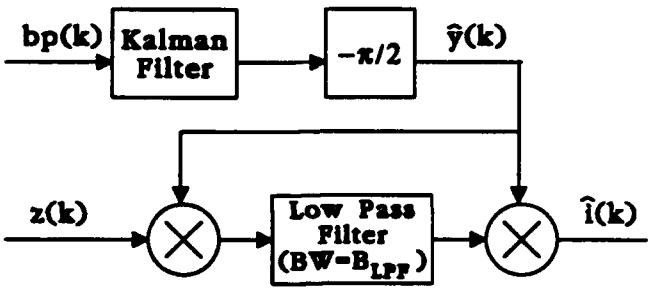

Figure 6: Block diagram of the interference estimator.

that it contributes insignificant aliased noise into the baseband region as a result of the sampling rate conditions discussed in Section 2.0. The term $\hat{I}'(k)$ is filtered by the low pass filter of bandwidth B_{LPF}, resulting in the estimate of the interference envelope, $\hat{I}(k)/\sqrt{2}$. Combining this with $\hat{y}(k)$ shown in Fig. 6 yields the estimate of the interference, i.e.,

$$\hat{i}(k) = \hat{I}(k)\cos[\omega_0 k + \hat{\theta}(k|k-1)], \tag{37}$$

which is subtracted from $z(k)$ to produce the error signal $e(k)$ as illustrated in Fig. 1. Because the input was coherently bandpass sampled at twice the chip rate, this error signal undergoes decimation and alternate sign reversal first, followed by correlation with the local PN code and bit detection. Several examples of the performance of the estimator will be presented next for the case of narrowband Gaussian noise interference.

5.0 SIMULATION RESULTS

This section describes the simulation conditions of tests which were conducted and presents examples of the performance of the excisor, including phase tracking, envelope estimation, and bit error rates. The parameters used in the simulations are listed in Table 1.

The modified Kalman algorithm, as alluded to by Eqs. (34) and (35), has been used in the simulations. The initial conditions were as follows:

$$\hat{\boldsymbol{x}}(-1) = E\{\hat{\boldsymbol{x}}(-1)\} = \begin{bmatrix} 0 \\ 0 \end{bmatrix} \tag{38}$$

$$\boldsymbol{V}_{\tilde{\boldsymbol{x}}}(-1) = E\{\tilde{\boldsymbol{x}}(-1)\tilde{\boldsymbol{x}}^t(-1)\} = \begin{bmatrix} 0.1 & 0.0 \\ 0.0 & 0.1 \end{bmatrix}. \tag{39}$$

The choice for the initial values in Eq. (39) is as follows. If the input to an integrator is zero mean white Gaussian noise of some variance, the output variance will increase linearly

Table 1: Simulation parameters..

Signal	Interference	Kalman Filter
$L = 20$ $E_b/N_0 = 10$ dB $E_c = 1$ unit $R_c = 1$ Hz	$B_i = 0.5\%$ to 5% of R_c $\omega_i{}^* = \omega_0$ I/S †(per chip) = 20 dB	$\alpha = 2\pi(.0003125)$ rad./sec. $K_w = 2\alpha$ $d(k) = d_0 e^{-.005k}$ ‡ $N/2 = 257$, 102, and 32.4 units

* Carrier frequency of interference.

† Interference-to-Signal ratio.

‡ A time-varying frequency deviation constant is used in one example.

with time, starting from an initial value of zero. If the output of the first integrator is applied to a second integrator, then the variance of the output of the second integrator will increase quadratically with time, also starting with an intial value of zero. To start the simulation with a positive definite covariance matrix, small positive values (i.e., 0.1) were inserted on the diagnal of Eq. (39). It should be noted too that the impact of the initial starting value will be transitory, eventually settling down to a steady state value. Finally, the bandwidths for the low pass filter B_{LPF} shown in Fig. 6 and used in determining the envelope of the interference, ranged from 0.1 Hz to 0.4 Hz.

The simulations were conducted using the baseband simulation model in [8], operated at the chip rate. Thus, the sampling rate was set at $f_s = R_c$, and the decimation and sign reversal operations were not required.

The phase and amplitude tracking capabilities of the interference estimator are shown in Figs. 8(a) and (b) for the simulation conditions in Table 1. The d profile for this test is in Fig. 7 and the bandwidth of the interference was .01 Hz. Referring to Fig. 8(a), for large values of d the phase noise is evident until at about 400 iterations, at which point the phase noise has decreased substantially; this indicates that the bandwidth of the Kalman filter has decreased. Observe also that initially, the algorithm exhibits some slippage, taking from 10 to 15 radians before it settles down to a tracking error of 2π radians after approximately 50 iterations. The initial slippage is due to d being initially too large. As d becomes too small, the algorithm eventually loses track because the rate of change of the phase is too fast for it (i.e., the bandwidth of the Kalman filter is too small). Figure 8(b) illustrates the estimate of the envelope of the interference. As d decreases,

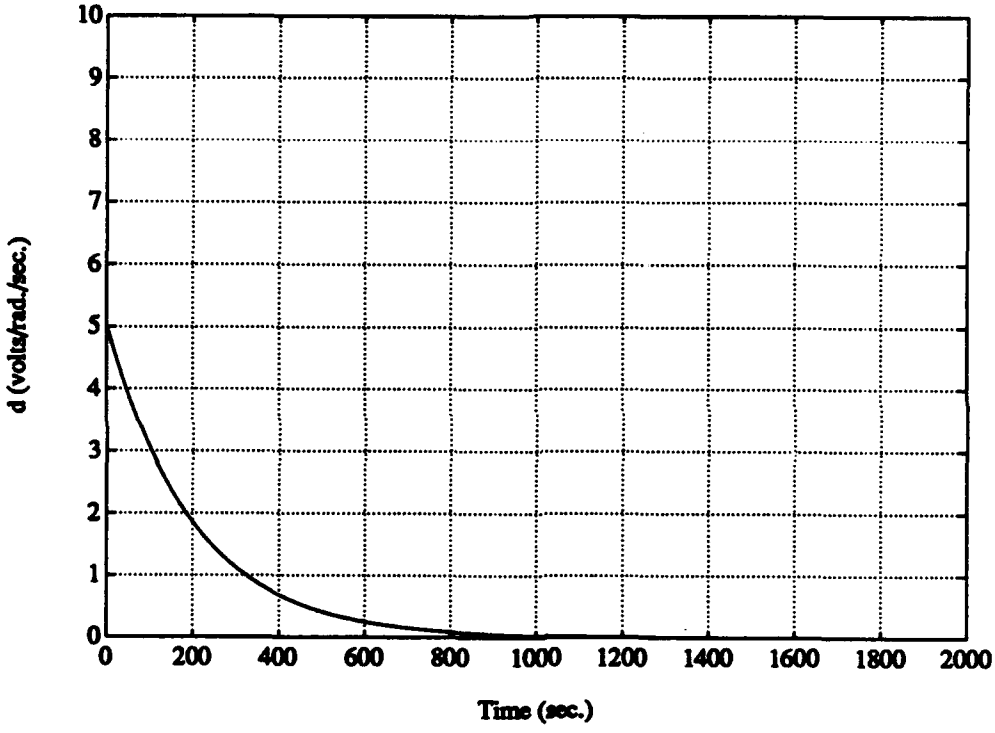

Figure 7: Profile of the frequency deviation constant d used in the phase and amplitude tracking tests.

$\hat{I}(k)$ appears to improve, until at approximately 1200 iterations, the estimate degrades substantially. The results in Fig. 8 suggest that an optimum value for d exists to achieve accurate tracking of the interferer.

The bit error rate as a function of several values of d is illustrated in Fig. 9 for an interference bandwidth $B_i = 0.005$ Hz and low pass filter bandwidths $B_{LPF} = .10$ and .20 Hz. As an example, the bit error rate decreases for increasing B_{LPF}, and the minimum bit error rate shifts to the right, implying that both the interference envelope and phase estimates are more accurate. One can keep increasing B_{LPF}; however, at some point, the bandwidth of the lowpass filter will be sufficient to provide a minimum bit error rate. Although not shown in Fig. (9), a bit error curve was generated for the case where B_{LPF} was set at .15 Hz, but it differed only slightly from the .20 Hz curve, suggesting that the optimum bandwidth for the lowpass filter was being approached. More simulations would have to be conducted to determine if bandwidths beyond .20 Hz would start to deteriorate the results.

Figure 10 illustrates the effect on bit error rate of an interferer with larger bandwidth, i.e., $B_i = .025$ Hz, for the same low pass filter bandwidths used in Fig. 9. The degradation in performance is quite evident. Comparing Figs. 9 and 10, for the same B_{LPF}, the required value for d increases as the interference bandwidth increases. Here too, more simulations would have to be conducted to determine if bandwidths beyond .20 Hz would continue to improve or deteriorate the results.

Finally, Fig. 11 exhibits the performance for $B_{LPF} = .20$ Hz and several interference bandwidths ranging from 0.005 to .025 Hz. As B_i increases, the bit error rate increases, and the bandwidth required by the Kalman filter also increases.

The effect on the bit error rate by modifying the carrier-to-noise ratio assumed in the interference model (i.e., differenct values of σ_v^2 or equivalently $N/2$) for $B_{LPF} = .20$ Hz and $B_i = .01$ Hz is illustrated in Fig. 12. Observe how the point at which the minimum bit error rate occurs shifts to the left for increasing gain (i.e., decreasing $N/2$). This implies that as the gain increases, the steady-state bandwidth of the Kalman filter increases for a given d, resulting in more phase noise. To compensate for this, a lower value of d is required. The important point to be made here is that one can select particular values for α and σ_v^2 and vary d to provide an adaptive capability.

The bit error rate performance as a function of E_b/N_0 for several interference bandwidths and optimum values of d, the latter of which were obtained from curves similar to those in Fig. 9 is illustrated in Fig. 13. The bandwidth B_{LPF} of the low pass filter was fixed at 0.4 Hz. Observe that for increasing values of B_i, the performance degrades. This degradation is due to two things: (a) increased levels of phase noise because of the

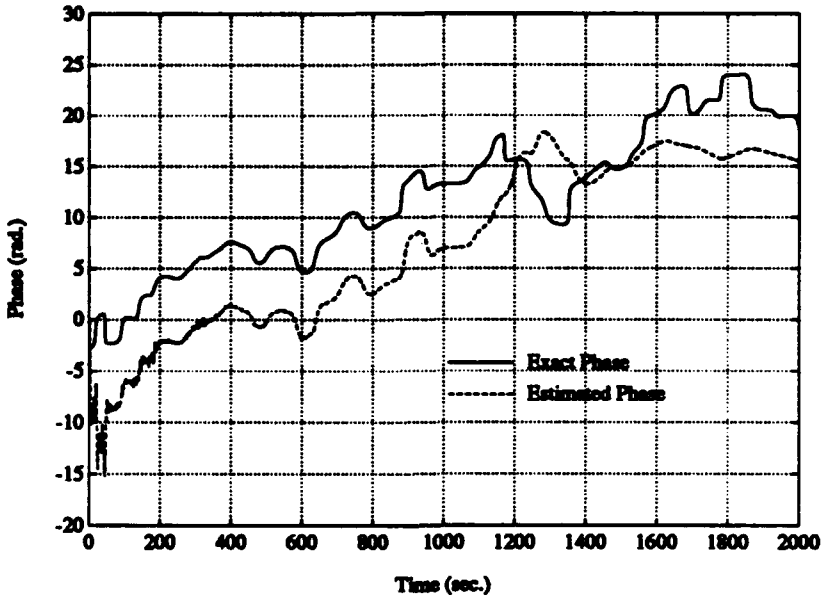

(a)

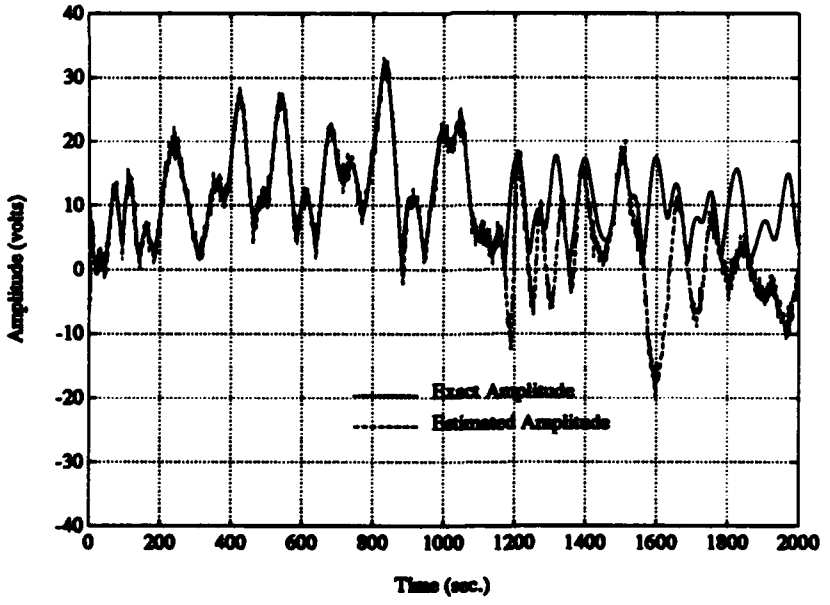

(b)

Figure 8: An example of the tracking ability of the interference estimator using the d profile in Fig. 7 ($B_i = 0.01$ Hz): (a) Phase; (b) Envelope.

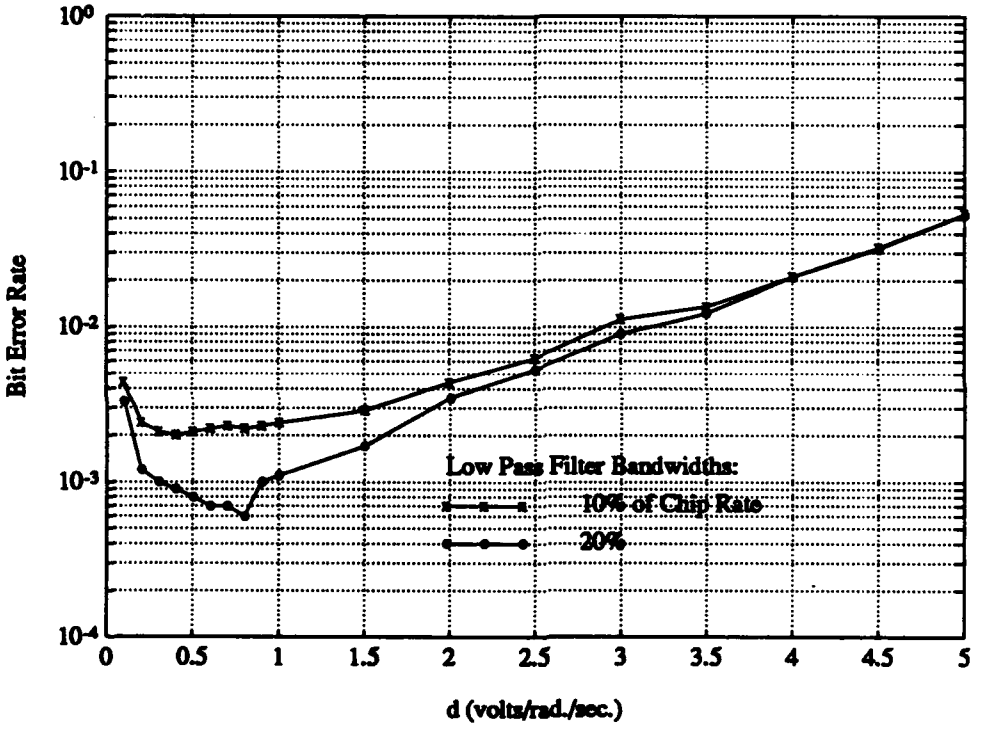

Figure 9: Bit error rates as a function of d and B_{LPF} for $B_i = 0.5\%$ of the chip rate.

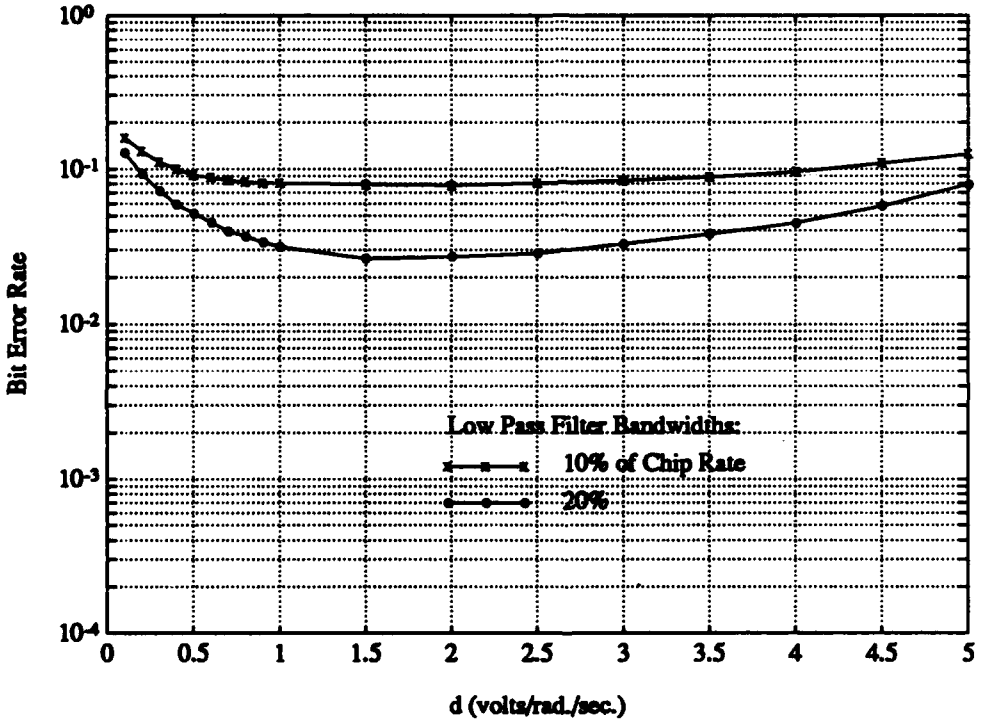

Figure 10: Bit error rates as a function of d and B_{LPF} for $B_i = 2.5\%$ of the chip rate.

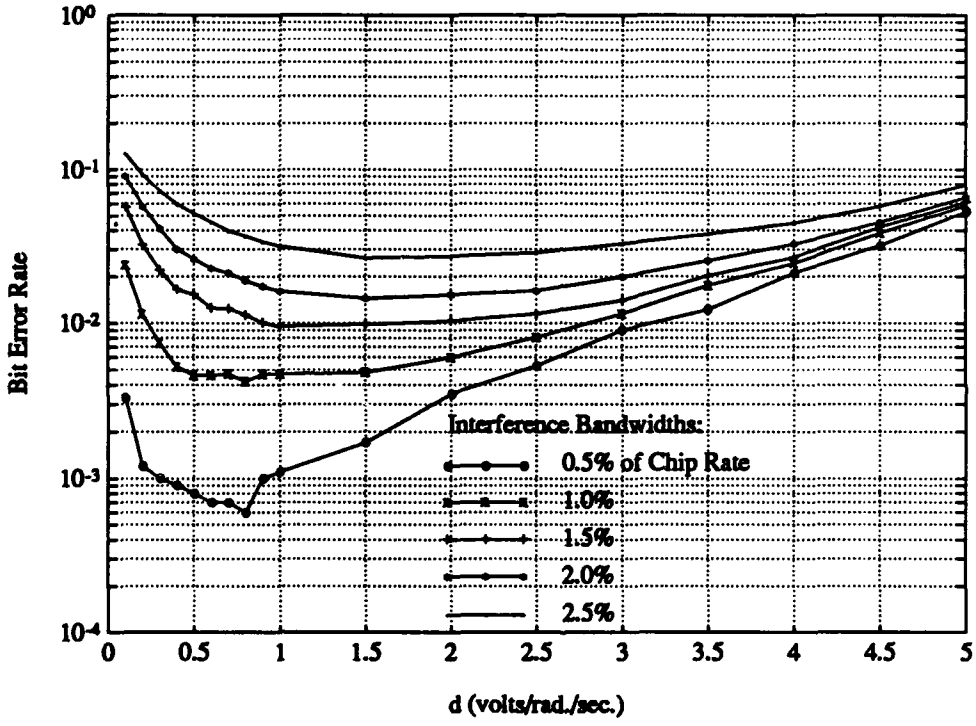

Figure 11: Bit error rates as a function of d and B_i for $B_{LPF} = 20\%$ of the chip rate.

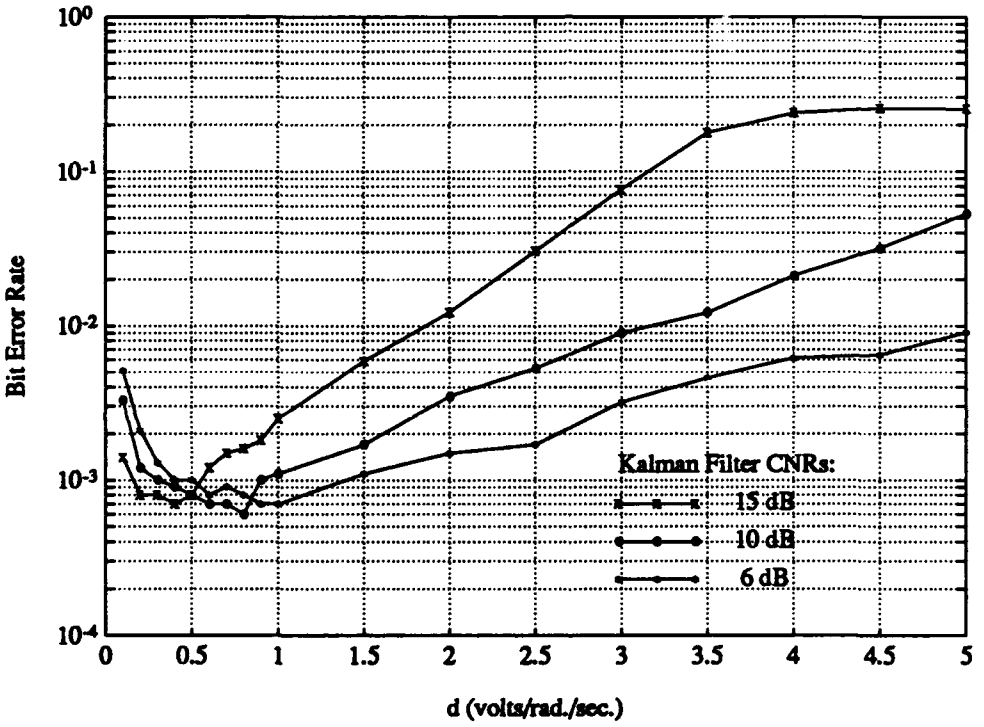

Figure 12: Bit error rate as a function of d and Kalman filter gain related to the carrier-to-noise ratio, $(CNR = 2/\alpha(N/2))$, in the interferer's "message" bandwidth, α.

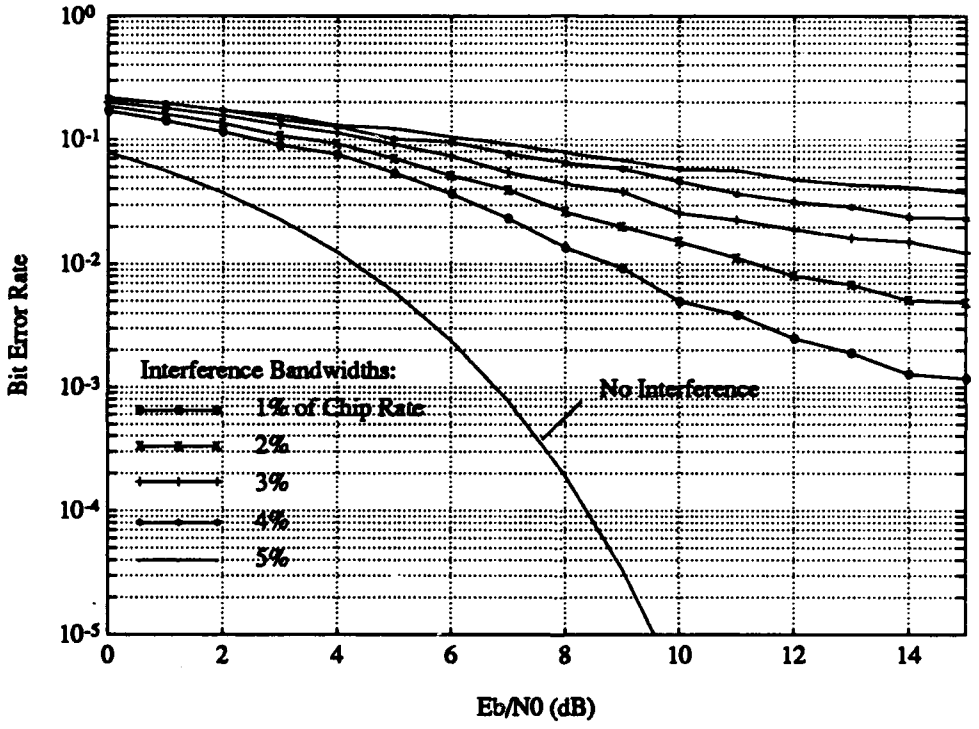

Figure 13: Bit error rate as a function of E_b/N_0 for several values of interference bandwidth, expressed as a percentage of the chip rate.

requirement for larger values of d to track the more rapidly varying interference (this translates into more residual interference at the output of the interference canceller in Fig. 1); and, (b) signal distortion at the output of the interference canceller.

6.0 ADAPTIVE ARCHITECTURES

To this point an excisor using a Kalman filter has been discussed, with several performance curves applied to a general form of interference, i.e., Gaussian narrowband interference. These results were obtained with a non-adaptive architecture. This section discusses three possible structures which would provide adaptive capabilities. The first is more appropriate for interferers with slowly varying envelopes; the second is the more general structure; and the third uses decision feedback, given an *a priori* data sequence to stabilize the Kalman parameters.

6.1 ARCHITECTURE 1 - CONSTANT ENVELOPE INTERFERER

The first architecture is illustrated in Fig. 14(a), which is an extension to Fig. 1. The main difference is the inclusion of an envelope detector which provides a reference signal for the Kalman filter. For large interference-to-signal-plus-noise ratio conditions, this is a reasonable approach.

How the reference signal $I_{ref}(k)$ is used by the interference estimator is illustrated in Fig. 14(b). The adaptive algorithm is intended to work as follows. Given that a narrowband interferer is present at some unknown frequency relative to the spread spectrum signal carrier, the frequency deviation constant d of the Kalman filter is set at a sufficiently large value so that the algorithm does not lock on to any signal; this value is determined from the parameters of the Kalman filter (i.e., α and σ_v^2) and its operating curves [8]. The frequency deviation constant d is then decreased at some rate using a profile similar to the one in Fig. 7. Before the Kalman filter locks on to the interferer, the error between the reference $I_{ref}(k)$ and $\hat{I}(k)$ will be large. It will remain so until d approaches the vicinity of the optimum value in a mean-squared context.

If the error is defined as

$$\epsilon(k) = I_{ref}(k) - \hat{I}(k), \tag{40}$$

then for a constant envelope interferer, and large interference-to-signal-plus-noise ratios,

$$(\theta(k) - \hat{\theta}(k|k-1))^2 \approx \epsilon(k)/I_{ref}. \tag{41}$$

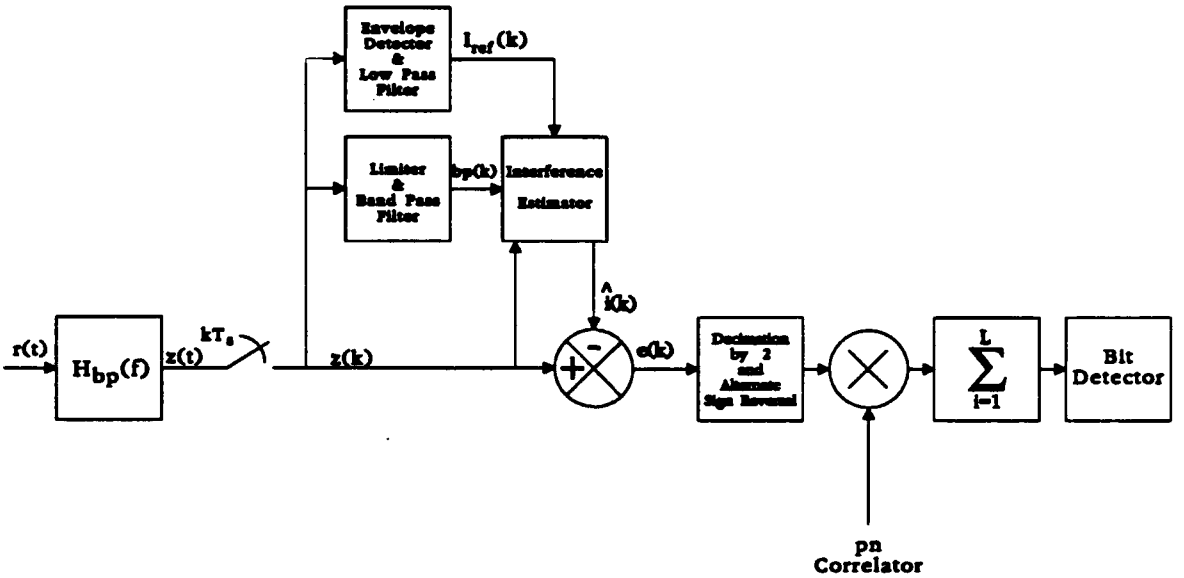

(a)

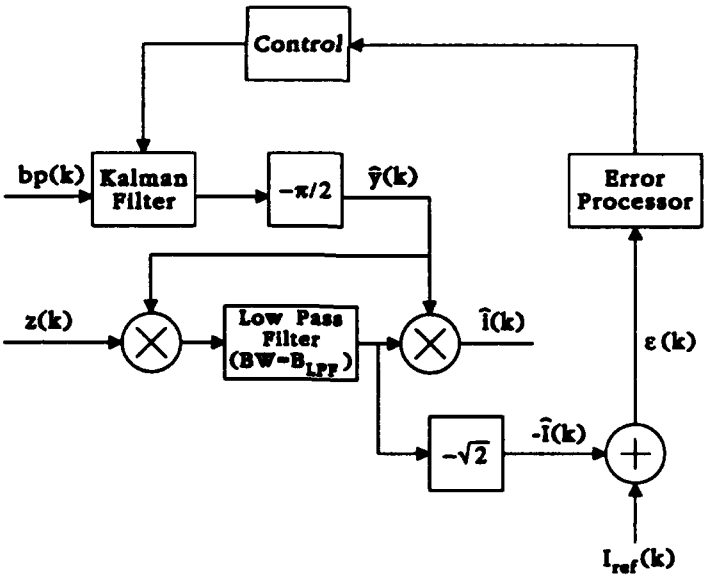

(b)

Figure 14: An adaptive architecture in which a reference signal $I_{ref}(k)$ is used by the Kalman algorithm: (a) System level diagram; (b) Amplitude estimator, error processor and controller.

This can be seen by noting from Eqs. (36) and (37), that the interference amplitude is

$$\hat{I} = I\cos(\theta(k) - \hat{\theta}(k|k-1)) + \textit{noise terms}. \tag{42}$$

By retaining the first two terms of an approximation to the cos term and assuming that $I_{ref} \approx I$, the desired result in Eq. (41) is obtained. The *Error processor* determines the mean of Eq. (41) while the box labelled *Control* monitors the mean-squared-error, continually looking for a minimum. If d gets too small, then the mean-squared-error starts to increase, implying that d must reverse its direction. An example of the performance of this excisor for the case of an FM interferer is in [15].

6.2 ARCHITECTURE 2 - GENERAL NARROWBAND INTERFERENCE

This architecture is shown in Fig. 15(a). The function which is minimized is $E\{\epsilon(k)^2\}$ preceding the despreader. This approach is similar to minimizing the squared error function resulting from the use of a linear predictor excisor [2]. For the linear predictor case, the function that is minimized is

$$E\{\epsilon^2(k)\} = E\{[(i(k) - \hat{i}(k)) + s(k) + n(k)]^2\}, \tag{43}$$

where

$$\begin{aligned} \hat{i}(k) &= a_1(i(k-1) + s(k-1) + n(k-1)) + \cdots \\ &+ a_m(i(k-m) + s(k-m) + n(k-m)). \end{aligned} \tag{44}$$

In Eq. (44), the a_i are the linear predictor coefficients of the excisor and m is the order of the linear predictor. Using the fact that $s(k) + n(k)$ is uncorrelated with $i(k) - \hat{i}(k)$, Eq. (43) can be rewritten as

$$E\{\epsilon^2(k)\} = E\{(i(k) - \hat{i}(k))^2\} + E\{(s(k) + n(k))^2\}. \tag{45}$$

The objective then, is to select the set of coefficients a_i, $i = 1, \cdots, m$ in Eq. (44) which minimizes Eq. (45) (i.e., the term $E\{(i(k) - \hat{i}(k))^2\}$) using, for example, the orthogonality principle [16].

For the Kalman filter excisor, an equation like Eq. (43) occurs, the main difference being that $\hat{i}(k)$ is correlated with $s(k) + n(k)$ since the *filter form* of the Kalman filter has been used. The result will be a degradation in performance. To circumvent this problem, one can use the *predictor form* of the Kalman filter, which would result in

an equation like Eq. (45). The trade-off here, however, is the fact that the interference estimate will be

$$\hat{i}(k) = \hat{I}(k-1)\cos(\omega_0 k + \hat{\theta}(k|k-2)) \tag{46}$$

as illustrated in Fig. 15(b). If it is assumed that the envelope varies slowly enough relative to the sampling rate so that $\hat{I}(k-1) \approx \hat{I}(k)$, then

$$\hat{i}(k) = \hat{I}(k)\cos(\omega_0 k + \hat{\theta}(k|k-2)). \tag{47}$$

The objective, using the Kalman filtering approach, would be to minimize the term $E\{(i(k) - \hat{i}(k))^2\}$ in Eq. (45) by adjusting d and B_{LPF} for fixed σ_v^2 and α.

For architectures 1 and 2, the signal-to-noise ratio at the output of the despreader can be shown to be [17]

$$SNR = \frac{L^2 E_c^2}{LE_c(N_0/2) + \sum_{k=1}^{L} E\{\Delta i(k)^2\}}, \tag{48}$$

where

$$\Delta i(k) = i(k) - \hat{i}(k), \tag{49}$$

and where it has been assumed that the filter/predictor form of the Kalman filter has been used. With the assumption that the noise at the output of the despreader is Gaussian, the resulting BER is, therefore,

$$P_b = \frac{1}{2} erfc\sqrt{SNR/2}, \tag{50}$$

where $erfc(x)$ is the complementary error function.

6.3 ARCHITECTURE 3 - DECISION FEEDBACK

The third architecture is illustrated in Fig. 16. The box shown as *Interference Estimator* uses the filter/predictor form (Fig. 15) without the delays following $bp(k)$ and $z(k)$. A training signal is provided initially to give time for the Kalman filter to stabilize without the signal being present, i.e., the input $z(k-1)$ during the training period has the known signal removed from it. The output before the limiter and bandpass filter is, therefore,

$$\begin{aligned} z'(k-1) &= z(k-1) - s(k-1) \\ &= i(k-1) + n(k-1). \end{aligned} \tag{51}$$

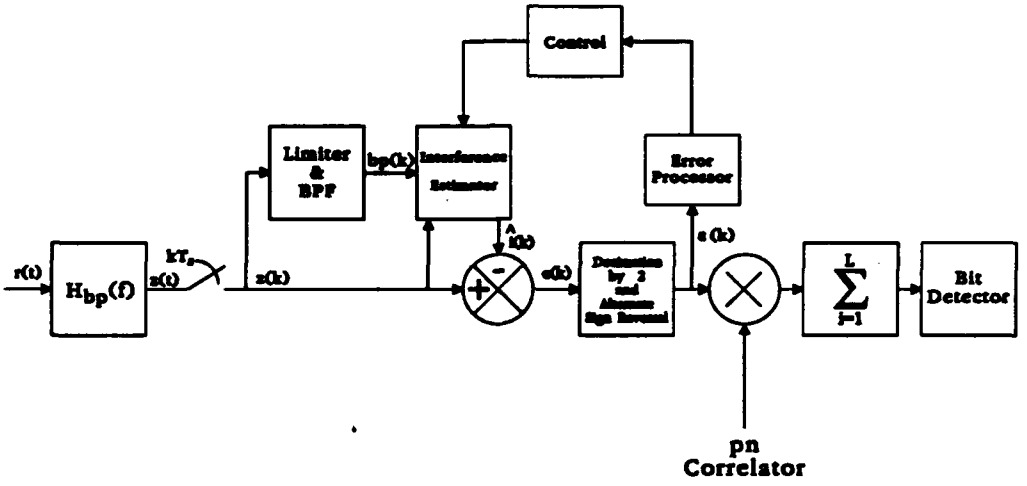

(a)

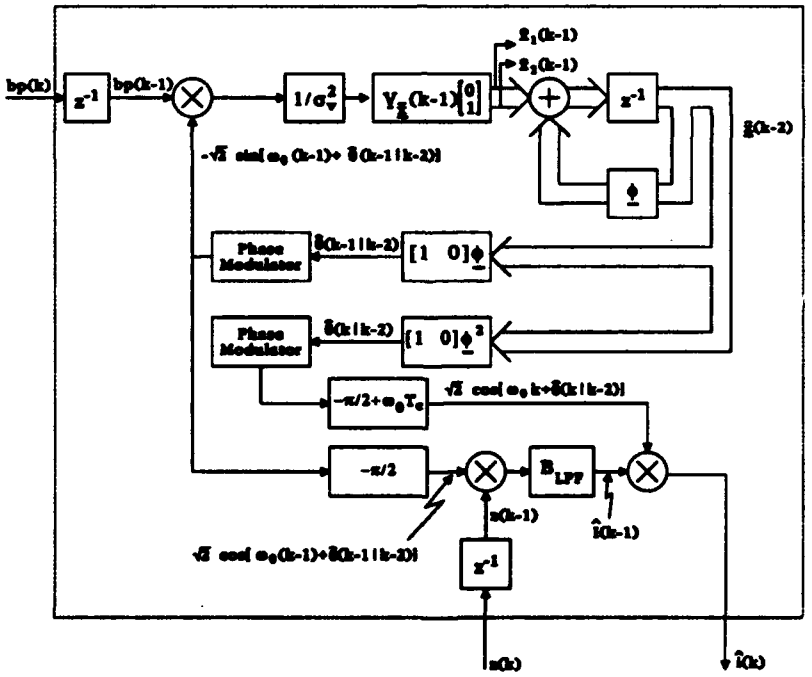

(b)

Figure 15: An adaptive architecture in which $E\{\epsilon^2(k)\}$ is minimized: (a) System level diagram; (b) Filter/Predictor form of the Kalman filter and amplitude estimator.

During the training period, the interference estimate will be more accurate. The output of the pn correlator, delayed by one chip, has the known signal also removed from it, resulting in the error signal

$$\epsilon(k-1) = n(k-1) + \Delta i(k-1), \tag{52}$$

where $\Delta i(k-1)$ is the residual interference. The function that is minizmized is $E\{\epsilon(k-1)^2\}$. When the training sequence is completed, the system shifts to the decision feedback mode, where the output of the bit detector produces a bit decision every T_c seconds, which is fedback. This feedback signal is respread and scaled to the chip energy level. It should be noted that the bit decision improves as the bit evolves over the L chips at the output of the summer following the pn correlation process; the summer is cleared every LT_c seconds.

Once the training sequence has passed, the performance will be a function of the bit error rate. During this mode of operation, the input to the limiter and bandpass filter will be

$$z'(k-1) = (s(k-1) - \hat{s}(k-1)) + n(k-1) + i(k-1). \tag{53}$$

As can be seen from Eq. (53), instances will occur (more so near the beginning of each bit) when the the first term will not be zero, resulting in some degradation in performance compared to the case when complete signal cancellation occurs. Further work is still required to assess this particular architecture.

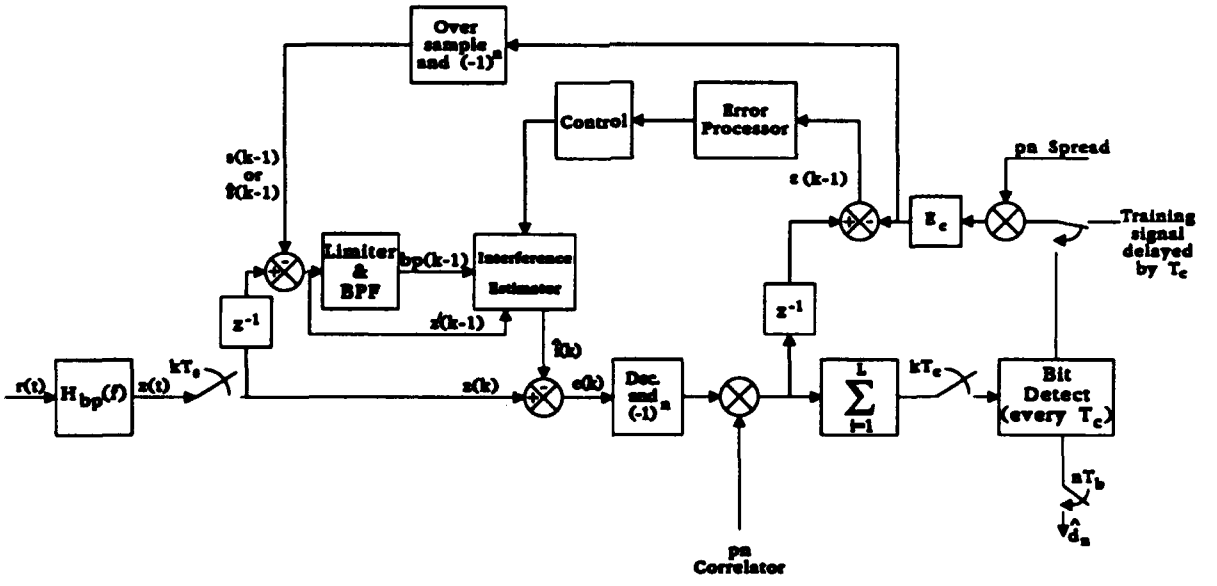

Figure 16: A decision-feedback excisor.

7.0 CONCLUDING REMARKS

A novel Kalman filtering approach has been presented for the suppression of interference in direct sequence spread spectrum communications systems. This approach differs from other time-modelling techniques based on Autoregressive methods.

Several bit error rate curves were obtained through simulation for the case of narrowband Gaussian noise interference. For increasing interference bandwidths, it was shown that performance degraded. It was also shown that performance was a function of the frequency deviation constant d of the Kalman filter, for fixed filter gain and "message bandwidth" α of the state space model. The bit error rate was more sensitive to the frequency deviation constant for quite narrow interference bandwidths (in the results the smallest bandwidth used was 0.005 Hz) than for larger bandwidths. For this latter case, there was a broad range of values for d which would suffice. It was also shown that performance was dependent on the bandwidth of the lowpass filter used in filtering the envelope of the interference.

The bit error rate results presented were not based on any particular adaptive architecture. The last section of this report presented three possible architectures, each one minimizing a different squared error function. The first architecture was more amenable to interferers with a constant or slowly varying envelope. The second was concerned with suppressing the more general interferer and involved minimizing the squared error function also used in the AR techniques. Finally, the third architecture incorporated decision feedback coupled with an initial training sequence. The main objective associated with this last approach was to reduce degrading effects due to the signal being present in estimating the interference.

Two areas of work remain to be completed. These include the development of theoretical bit error rate curves for the three architectures, and the assessment of the decision feedback architecture through computer simulation.

REFERENCES

[1] F. M. Hsu and A. A. Giordano, "Digital whitening techniques for improving spread spectrum communications performance in the presence of narrowband jamming and interference," *IEEE Transactions on Communications*, vol. 26, pp. 209–216, February 1978.

[2] J. W. Ketchum and J. G. Proakis, "Adaptive algorithms for estimating and suppressing narrowband interference in PN spread-spectrum systems," *IEEE Transactions on Communications*, vol. 30, pp. 913–924, May 1982.

[3] L. B. Milstein, "Interference rejection techniques in spread spectrum communications," *Proceedings of the IEEE*, vol. 76, pp. 657–671, June 1988.

[4] J. P. Burg, "Maximum entropy spectrum analysis," in *Modern Spectrum Analysis* (D. G. Childers, ed.), pp. 34–41, New York:IEEE Press, 1978.

[5] B. Widrow, J. M. McCool, M. G. Larimore, and C. R. Johnson, "Stationary and nonstationary learning characteristics of the LMS adaptive filter," *Proceedings of the IEEE*, vol. 64, pp. 1151–1161, August 1976.

[6] S. L. Marple, "A new autoregressive spectrum analysis algorithm," *IEEE Transactions on Acoustics, Speech, and Signal Processing*, vol. 28, pp. 441–454, August 1980.

[7] J. M. Cioffi and T. Kailath, "Fast, recursive-least-squares transversal filters for adaptive filtering," *IEEE Transactions on Acoustics, Speech, and Signal Processing*, vol. 32, pp. 304–337, April 1984.

[8] D. R. Polk and S. C. Gupta, "Quasi–optimum digital phase–locked loops," *IEEE Transactions on Communications*, vol. 21, pp. 75–82, January 1973.

[9] C. N. Kelly and S. C. Gupta, "The digital phase-locked loop as a near-optimum FM demodulator," *IEEE Transactions on Communications*, vol. 20, pp. 406–411, June 1972.

[10] M. J. Bouvier, Jr., "The rejection of large CW interferers in spread spectrum systems," *IEEE Transactions on Communications*, vol. 26, pp. 254–256, February 1978.

REFERENCES

[11] D. F. Liang, "Comparisons of nonlinear recursive filters for systems with non-negligible nonlinearities," in *Control and Dynamic Systems: Advances in Theory and Applications-Volume 20* (C. T. Leondes, ed.), Academic Press, 1983.

[12] A. Blanchard, *Phase-Locked Loops.* New York:John Wiley and Sons, 1976.

[13] A. P. Sage and J. L. Melsa, *Estimation Theory with Applications to Communications and Control.* New York:McGraw-Hill, 1971.

[14] H. L. Van Trees, *Detection, Estimation, and Modulation-Part2: Nonlinear Modulation Theory.* New York:John Wiley and Sons, 1971.

[15] B. W. Kozminchuk and A. U. H. Sheikh, "A Kalman filtering technique for suppressing jammers in direct sequence spread spectrum communication systems," in *Queens 50th Biennial Symposium on Communications*, pp. 5–8, June 1990. Kingston, Ontario.

[16] A. Papoulis, *Probability, Random Variables, and Stochastic Processes.* McGraw–Hill, 1984.

[17] B. W. Kozminchuk, "Excision techniques in direct sequence spread spectrum communication systems," Technical Report 1047, Defence Research Establishment Ottawa, Ottawa, Ontario, Canada, K1A 0Z4, 1990.

DOCUMENT CONTROL DATA

(Security classification of title, body of abstract and indexing annotation must be entered when the overall document is classified)

1. ORIGINATOR (the name and address of the organization preparing the document. Organizations for whom the document was prepared, e.g. Establishment sponsoring a contractor's report, or tasking agency, are entered in section 8.)

NATIONAL DEFENCE
DEFENCE RESEARCH ESTABLISHMENT OTTAWA
SHIRLEY BAY, OTTAWA, ONTARIO K1A 0K2 CANADA

2. SECURITY CLASSIFICATION (overall security classification of the document, including special warning terms if applicable)

UNCLASSIFIED

3. TITLE (the complete document title as indicated on the title page. Its classification should be indicated by the appropriate abbreviation (S,C or U) in parentheses after the title.)

KALMAN FILTER-BASED ARCHITECTURES FOR INTERFERENCE EXCISION (U)

4. AUTHORS (Last name, first name, middle initial)

KOZMINCHUK, BRIAN W.

5. DATE OF PUBLICATION (month and year of publication of document)	6a. NO. OF PAGES (total containing information. Include Annexes, Appendices, etc.)	6b. NO. OF REFS (total cited in document)
DECEMBER 1991	35	17

7. DESCRIPTIVE NOTES (the category of the document, e.g. technical report, technical note or memorandum. If appropriate, enter the type of report, e.g. interim, progress, summary, annual or final. Give the inclusive dates when a specific reporting period is covered.)

DREO TECHNICAL REPORT

8. SPONSORING ACTIVITY (the name of the department project office or laboratory sponsoring the research and development. Include the address.)

NATIONAL DEFENCE
DEFENCE RESEARCH ESTABLISHMENT OTTAWA
SHIRLEY BAY, OTTAWA, ONTARIO K1A 0K2 CANADA

9a. PROJECT OR GRANT NO. (if appropriate, the applicable research and development project or grant number under which the document was written. Please specify whether project or grant)	9b. CONTRACT NO. (if appropriate, the applicable number under which the document was written)
041LK11	

10a. ORIGINATOR'S DOCUMENT NUMBER (the official document number by which the document is identified by the originating activity. This number must be unique to this document.)	10b. OTHER DOCUMENT NOS. (Any other numbers which may be assigned this document either by the originator or by the sponsor)
DREO REPORT 1118	

11. DOCUMENT AVAILABILITY (any limitations on further dissemination of the document, other than those imposed by security classification)

(X) Unlimited distribution
( ) Distribution limited to defence departments and defence contractors; further distribution only as approved
( ) Distribution limited to defence departments and Canadian defence contractors; further distribution only as approved
( ) Distribution limited to government departments and agencies; further distribution only as approved
( ) Distribution limited to defence departments; further distribution only as approved
( ) Other (please specify):

12. DOCUMENT ANNOUNCEMENT (any limitation to the bibliographic announcement of this document. This will normally correspond to the Document Availability (11). However, where further distribution (beyond the audience specified in 11) is possible, a wider announcement audience may be selected.)

UNCLASSIFIED

SECURITY CLASSIFICATION OF FORM

13. ABSTRACT (a brief and factual summary of the document. It may also appear elsewhere in the body of the document itself. It is highly desirable that the abstract of classified documents be unclassified. Each paragraph of the abstract shall begin with an indication of the security classification of the information in the paragraph (unless the document itself is unclassified) represented as (S), (C), or (U). It is not necessary to include here abstracts in both offical languages unless the text is bilingual).

(U) This report presents a novel Kalman filtering approach to the suppression of narrowband interference from direct sequence spread spectrum communications systems. The algorithm is based on the digital phase-locked loop Kalman filter. Because the interference is assumed to be much stronger than either the signal or noise, the Kalman filter locks onto a function related to the interference. The net result is an estimate of the phase of the interference and its amplitude. The algorithm is characterized through computer simulation for the case of narrowband Gaussian noise interference. Examples of the phase- and envelope-tracking capabilities of the algorithm are presented, followed by bit error rate curves for interference bandwidths ranging from 0.5% to 5.0% of the chip rate of the spread spectrum signal. The report concludes with three adaptive architectures. The first is suitable for constant envelope interference; the second is a more general structure; and the third incorporates a decision-feedback structure accompanied with a training sequence.

14. KEYWORDS, DESCRIPTORS or IDENTIFIERS (technically meaningful terms or short phrases that characterize a document and could be helpful in cataloguing the document. They should be selected so that no security classification is required. Identifiers, such as equipment model designation, trade name, military project code name, geographic location may also be included. If possible keywords should be selected from a published thesaurus, e.g. Thesaurus of Engineering and Scientific Terms (TEST) and that thesaurus-identified. If it is not possible to select indexing terms which are Unclassified, the classification of each should be indicated as with the title.)

KALMAN FILTERING
SPREAD SPECTRUM
ADAPTIVE FILTERING
INTERFERENCE SUPPRESION
EXCISION
ESTIMATION THEORY

UNCLASSIFIED

SECURITY CLASSIFICATION OF FORM